GRID-INTEGRATION IMPROVEMENT FOR PMSG WIND TURBINE SYSTEM UNDER GRID VOLTAGE DISTURBANCES

Van Tan Luong*, Ho Nhut Minh+
* Ho Chi Minh city University of Food Industry
+ Posts and Telecommunications Institute of Technology

Abstract - In this work, an enhanced control method for a grid-connected voltage-source converter of permanent-magnet synchronous generator (PMSG) wind turbine system under unbalanced and distorted grid voltages is introduced. With the proposed method, the grid current regulators based on proportional-integral and resonant (PIR) control are applied to order to mitigate the current distortion flowing into the grid. The validity of this control scheme has been verified by the simulation of the 2MW-PMSG wind turbine system.

Keywords - Grid converter, voltage unbalance and distortion, proportional-resonant (PR) control, wind turbine.

I. INTRODUCTION

In recent years, three-phase voltage-source pulse-width modulation (PWM) converters are important components in industrial applications of power conversion such as alternating current (AC)-machine drive, uninterruptible power supplies (UPS), and integration of renewable energy sources to the electricity grid [1 - 3]. They can give the constant direct current (DC)-link voltage, sinusoidal input current, unity power factor operation, and bi-directional power flow [4]. In particular, the function of the PWM converter is important for grid connection since the utility operator requires to satisfy the grid code and to avoid the islanding operation.

Several methods have been suggested for controlling the grid-connected three-phase converter to mitigate the current distortion due to the unbalance and harmonics in the grid voltage. In the cases of a single current control loop, the grid converters can not give good performance in unbalanced grid voltage conditions due to the appearance of a second-order harmonic voltage component at the DC-link bus [4]. Also, the fifth, seventh and higher-order harmonics produced by nonlinear loads cause the grid voltage distortion [5]. The harmonic distortion causes not only the grid power oscillations, but also possibly a failure to the converter [4 - 5]. To handle these issues, a double-frame current control scheme has been applied for separately controlling the positive- and negative sequence current components to mitigate the second-order harmonic voltage component [4 - 5]. However, the current control performance has been still influenced by the fifth- and seventh-order harmonics since the bandwidth of the current control loop is high.

A phase-locked loop (PLL) system is often used to detect the phase angle of the AC grid voltage in the power quality fields, such as the reactive power compensator, uninterruptable power supply and active power filters. To estimate the frequency or the phase angle of the three-phase system under unbalanced and distorted grid conditions, several methods have been suggested in the literatures [6 - 8]. A method using the PLL based on the synchronous reference frame (SRF-PLL) has been obtained by using Park's transformation [6-7]. With this method, the SRF-PLL translates the three-phase voltage vector from the abc natural reference frame to the dq rotating reference frame. The angular position of this dq reference frame is controlled by a feedback loop that regulates the q component to zero. However, the limitation of the PLL bandwidth is not the most effective solution to extract the positive sequence component from the unbalanced three-phase voltages resulting from an asymmetrical grid fault. This problem is improved by using decoupled double synchronous reference frame-PLL (DDSRF-PLL) [8]. This DDSRF-PLL based on employing two synchronous reference frames, rotating with positive and negative synchronous speeds, respectively. The usage of this double synchronous reference frame allows decoupling of the effect of the negative-sequence voltage component on the dq signals detected by the synchronous reference frame rotating with positive angular speed, and vice versa, which makes grid synchronization possibly accurate even under unbalanced grid faults. However, during the unbalanced grid faults, the power converter controllers can also be implemented on the stationary reference frame by using resonant controllers. In this case, the grid voltage phase angle is not the most important variables of the synchronization – the grid frequency is.

Resonant controllers are selected as an alternative control structure for harmonic control at rotor-side

Corespondence: Van Tan Luong
Email: luonghepc@gmail.com
Manuscript received 5/6/2021, revised: 5/9/2021, accepted: 27/10/2021

converter of doubly-fed induction generator (DFIG). The use of resonant controllers aims to obtain high bandwidth at certain frequencies and also removes current harmonics in the DFIG during grid voltage distortion [9]. In [10], both the fifth- and seventh-order harmonics in the stator output voltage are removed by a resonant controller for a stand-alone of the DFIG. By using resonant controllers, the steady-state errors at the selected resonant frequencies have been eliminated. However, the case of grid voltage unbalance has been not considered in the system. Also, the grid voltage phase angle related to PLL method which directly affects the grid synchronization has been ignored to control system.

In this paper, the PIR current controllers are proposed to mitigate the unbalanced and distorted components of the grid current from the system. Also, a second-order generalized integrator (SOGI) is applied to a grid-side converter to achieve precise phase angle detection. In addition, the resonant controllers are also used to damp the resonant grid current components at the resonant frequency, in which the resonant grid currents are extracted by band-pass filters (BPF). The simulation results for the 2 MW-PMSG wind turbine system are provided to verify the effectiveness of the proposed method.

II. SYSTEM MODELING

A. SYSTEM DESCRIPTION

Figure 1 shows configuration of the PMSG wind turbine system, which is connected to the grid through full neutral point clamping (NPC) three-level back-to-back PWM converters, where ega, egb, and egc represent the source phase voltages, and LCL and C denote the line inductance-capacitance-inductance and the DC-link capacitance, respectively. The resonant frequency (fr) of the LCL filters is given by [11 - 12].

$$f_r = \frac{1}{2\pi}\sqrt{\frac{L_f + L_g}{C_f L_f L_g}} \qquad (1)$$

The parameters of the *LCL* filters are determined from the requirements of the current ripples on the grid and converter sides. Also, the resonant frequency should be in a range between ten times the grid frequency and a half of the switching frequency [12 - 13]

B. MATHEMATICAL EQUATION

Neglecting the filter capacitor, the grid converter can be represented in the dq-synchronous reference

frame as [4]

$$\begin{aligned} E_{de} &= R_t I_{de} + L_t \frac{dI_{de}}{dt} + V_{de} - \omega_e L_t I_{qe} \\ E_{qe} &= R_t I_{qe} + L_t \frac{dI_{qe}}{dt} + V_{qe} - \omega_e L_t I_{de} \end{aligned} \qquad (2)$$

where $L_t = L_f + L_g$ and $R_t = R_f + R_g$ are the summation of the grid and converter filter inductances and its equivalent series resistance, respectively, ω_e is the angular frequency of the grid voltage, E_{dqe} is the dq-axis grid voltages and V_{dqe} is the *dq*-axis converter voltages.

III. EFFECT OF GRID VOLTAGE DISTURBANCES

Since the fifth- and seventh-order harmonic components are significant, the unbalanced components and the fifth- and seventh-order harmonics in the grid voltage are considered in this work. The grid voltage vector ($e^s(t)$) in the stationary reference frame is expressed as

$$e^s(t) = (E_{dq}^{1+} e^{j\omega_e t} + E_{dq}^{1-} e^{-j\omega_e t} + E_{dq}^{5} e^{-j5\omega_e t} + E_{dq}^{7} e^{j7\omega_e t}) \quad (3)$$

where E_{dq}^{1+}, E_{dq}^{1-}, E_{dq}^{5}, and E_{dq}^{7} are the magnitude of the positive-, negative-, fifth- and seventh-order components, respectively.

The grid voltage vector ($e^e(t)$) in the synchronous reference frame rotating in the direction of the positive sequence is expressed as.

$$\begin{aligned} e^e(t) &= e^s(t) \cdot e^{-j\omega_e t} \\ &= (E_{dq}^{1+} + E_{dq}^{1-} e^{-j2\omega_e t} + E_{dq}^{5} e^{-j6\omega_e t} + E_{dq}^{7} e^{j6\omega_e t}) \end{aligned} \qquad (4)$$

From (4), the grid voltage contains DC-quantities for the positive-sequence component and the second-order harmonics for the negative-sequence component, while the fifth- and seventh-order harmonics appear as the sixth-order harmonic component.

The second-order and sixth-order components of the grid voltages cause the distortion of the grid current [14]. Thus, it is desired that the distorted and unbalanced grid currents need to be mitigated for power quality problems as well as safe operation of the grid-connected converter.

IV. PLL UNDER UNBALANCED AND DISTORTED GRID VOLTAGE

Figure 2 shows the block diagram of the PLL based on the SOGI in stationary reference frame for the grid-side converter. First, the three-phase voltage vector (v'_α) from the *abc* natural reference frame to the *αβ* stationary reference frame. Then, two SOGIs are in charge of generating the direct and in-quadrature signals for the α and β components of the input vector (v'_α and qv'_α, v'_β and qv'_β). Next, these signals are applied to calculate the positive- and negative-sequence components in the *αβ* reference frame ($v^{+'}_{\alpha\beta}$ and $v^{-'}_{\alpha\beta}$) of the grid voltages [15 - 17]. As observed in this figure, the phase angle (θ) extracted from the positive-sequence component of the grid voltages is used for the voltage and current transformations. The SOGI-based method gives a good estimation performance under distorted and unbalanced grid voltage conditions.

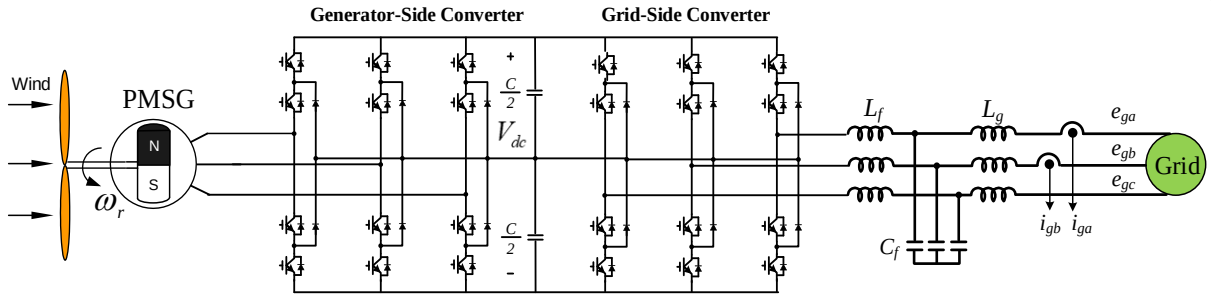

Figure 1. *Circuit configuration of PMSG wind turbine system.*

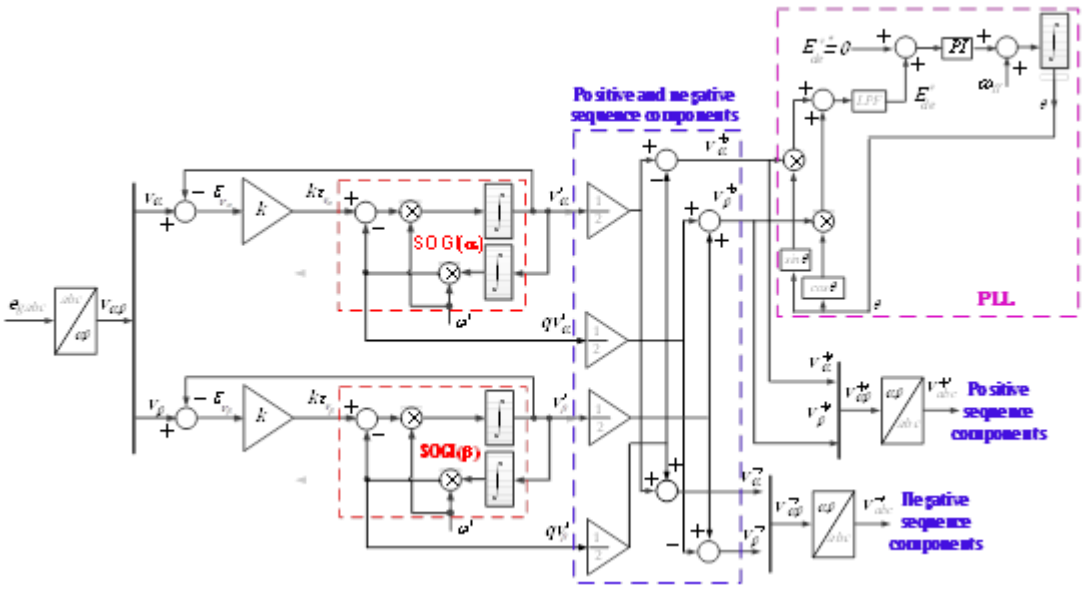

Figure 2. *Block diagram of SOGI-PLL.*

V. PROPOSED CONTROL SCHEME FOR GRID-SIDE CONVERTER

A closed-loop current control scheme is described in Figure 3. The *s*-domain open-loop transfer function of the PIR current controller is defined as follows:

$$G_0(s) = k_p + \frac{k_i}{s} + \sum_{h=2,6} \frac{k_{ph}s^2 + k_{rh}s}{s^2 + (h\omega_e)^2} \quad (5)$$

where k_p, k_i, k_{ph} and k_{rh} are the gain parameters of the current controller.

The closed-loop transfer function of the control scheme is given by:

$$G_c(s) = \frac{I_{dqe}(s)}{I^*_{dqe}(s)} = \frac{G_0(s)}{(L_t s + R_t) + G_0(s)} \quad (6)$$

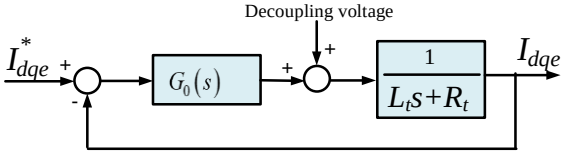

Figure 3*. Block diagram of the proposed PIR current controller.*

As aforementioned, the design of the current controller was implemented based on the Naslin polynomial technique which was used to determine the controller gains. The characteristic polynomial of the closed-loop transfer function in (6) can be calculated as:

$$D(s) = (L_t s + R_t)s\left[s^2 + (2\omega_e)^2\right] + k_p s\left[s^2 + (2\omega_e)^2\right] + k_i\left[s^2 + (2\omega_e)^2\right] + k_{p2}s^3 + k_{r2}s^2 \quad (7)$$

The parameters of the controller are calculated based on the fourth-order Naslin polynomial as:

$$N(s) = \alpha_0\left[1 + \frac{s}{\omega_n} + \frac{s^2}{\alpha\omega_n^2} + \frac{s^3}{\alpha^3\omega_n^3} + \frac{s^4}{\alpha^6\omega_n^4}\right] \quad (8)$$

where α is the characteristic ratio and ω_n is the Naslin frequency.

Matching the coefficients for (7) and (8) gives the controller gains to be used in the proposed current controller as follows:

$$\begin{cases} \alpha_0 = L_t\alpha^6\omega_n^4 \\ k_p = \dfrac{L_t\alpha^6\omega_n^3}{4\omega_e^2} - R_t \\ k_i = \dfrac{L_t\alpha^6\omega_n^4}{4\omega_e^2} \\ k_{p2} = L_t\alpha^3\omega_n - \dfrac{L_t\alpha^6\omega_n^3}{4\omega_e^2} \\ k_{r2} = L_t\alpha^5\omega_n^2 - 4\omega_e^2 L_t - \dfrac{L_t\alpha^6\omega_n^4}{4\omega_e^2} \end{cases} \quad (9)$$

The characteristic ratio of the Naslin polynomial is generally chosen to be $\alpha = 2$. Thus, the appropriate gains of the proposed current controller are achieved by (9). In this work, these gain parameters used for the simulation process are k_p = 0.997, k_i = 300.909, k_{p2} = k_{p6} = 1.003, k_{r2}= k_{r6} = 461.879.

Figure 4 shows the control block diagram of the proposed method for the grid-side converter, which consists of an outer DC-link voltage control loop and an inner current control loop. As for the first loop, the DC-link voltage of the back-to-back PWM converter in the wind power system must be controlled constant to deliver the generated power from the generator to the grid. The latter loop one allows to regulate the grid currents to be sinusoidal, regardless of the unbalanced and distorted grid voltages, in which the components of the unbalanced and distorted grid current must be controlled to zero. To design the *LCL* filter, its resonant frequency should be selected to be lower than a half of the switching frequency.

As mentioned previously, in order to control the current components under unbalanced and distorted grid voltage conditions, the negative-sequence and fifth- and seventh-order harmonic components of grid current in the dq coordinates behave as AC components pulsating at $2\omega_e$ and $6\omega_e$, respectively. Thus, the PIR controller is capable of simultaneously regulating both the positive- and negative sequence currents and, fifth- and seventh-order harmonic currents in the dq coordinates by forcing their steady-state error to be zero. Also, the resonant component of the grid currents is damped to zero by the resonant regulators at the resonant frequency, in which these gain parameters applied for the simulation process are k_{r5} = k_{r7} = 5 by trial and error method. In this research, the resonant frequency of the *LCL* filters is chosen as 830 Hz. To extract the resonant component of the grid currents, the cut-off frequency and bandwidth of the BPF are selected to be 830 Hz and 200 Hz, respectively.

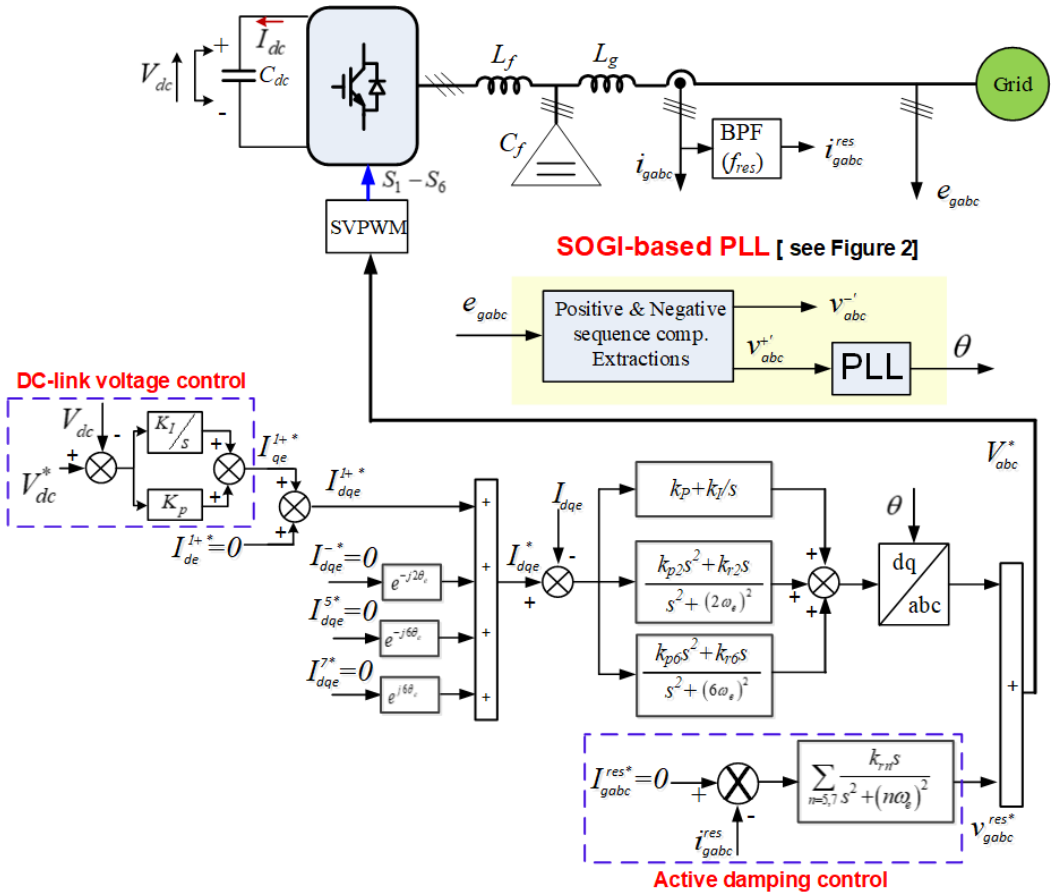

Figure 4. *Proposed control block diagram of overall system.*

VI. SIMULATION RESULSTS

To verify the effectiveness of the proposed method, the simulation using PSIM software has been carried out for 2MW - PMSG wind turbine. The parameters of the grid PWM converter and generator are listed in Table 1 and 2, respectively. The DC-link voltage is controlled at 1.2 kV; the DC-link capacitance is 0.1 F; the switching frequency is 2.5 kHz and the grid voltage is 690 V/60 Hz.

Table 1. *Parameters of grid PWM converter*

Parameters	Values
Rated power	2 MW
Grid voltage	690 V/60 Hz
Grid/converter filter inductances	0.3/0.03 mH
Shunt filter capacitance	670 μF

Table 2. *Parameters of 2 MW-PMSG*

Parameter	Values
Rated power	2 MW
Grid voltage	690 V
Stator voltage/frequency	690 V/60 Hz
Stator resistance	0.008556 Ω
d-axis inductance	0.00359 H
q-axis inductance	0.00359 H

Figure 5 shows the performance of the PLL in the two cases: distorted grid voltages (see Figure 5(A)) and unbalanced and distorted grid voltages (see Figure 5(B)). Figure 5(a) shows the grid voltages (e_{gabc}), which contain the 5% fifth- and seventh-order harmonics at 0.1 s (from 3.95 s to 4 s and from 4.1 s to 4.15 s) and both the 5% fifth- and seventh-order harmonics and the 15 % drop in two phase voltages at 0.1 s (from 4 s to 4.1 s). The wind speed (V_{wind}) is assumed to be 8.2 m/s for easy investigation.

In case of the distorted grid voltages as shown in Figure 5A(a), the positive-sequence components of the grid voltages which are extracted by the SOGI method, are sinusoidal. The positive-sequence components of the grid voltage in *dq*-axis are illustrated in Figure 5A(c), in which the *d*-axis component is set to be zero for the grid voltage orientation. Figure 5A(d) shows the phase angle of the positive sequence voltage component, which is well estimated under distorted grid voltage.

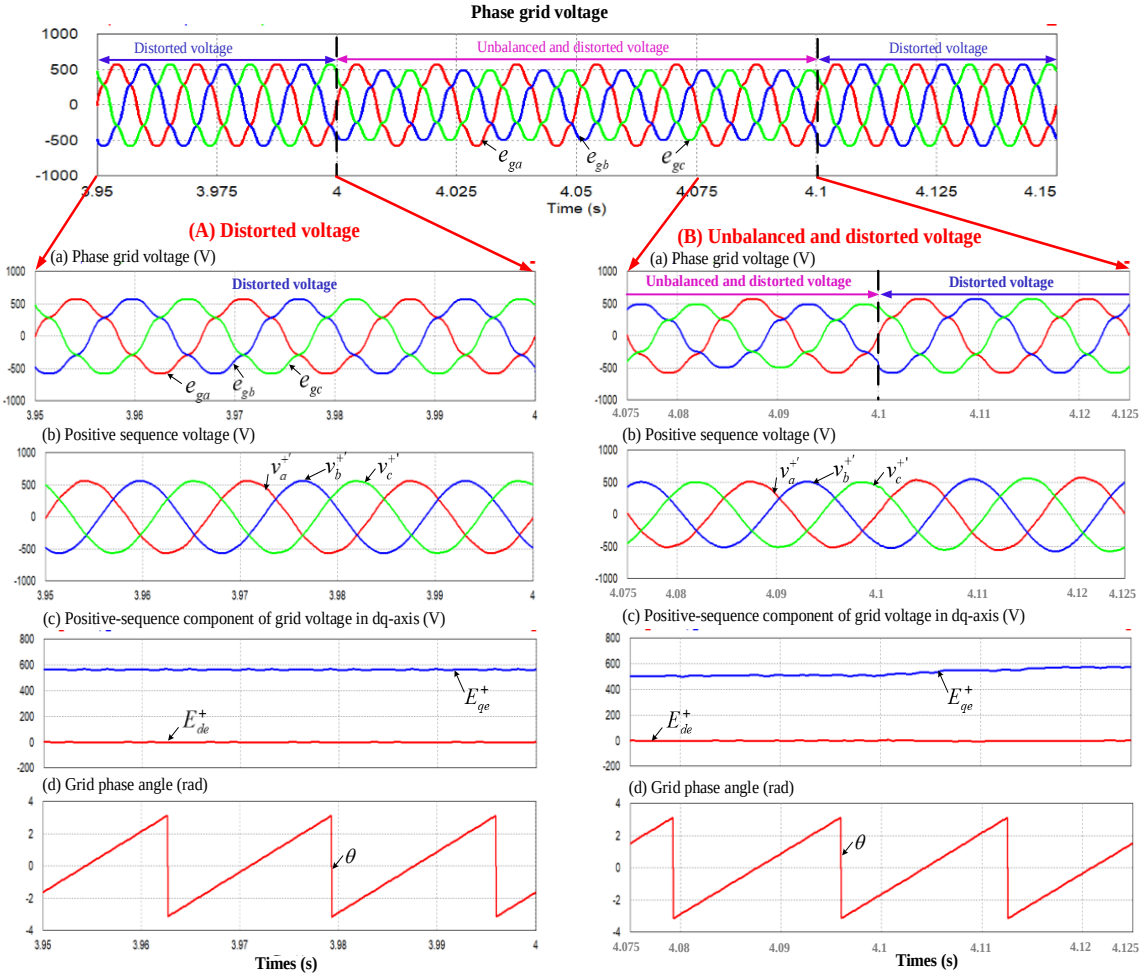

Figure 5. *PLL performance in two cases: (A). Distorted voltage and (B). Unbalanced and distorted voltage.*

In case of the unbalanced and distorted grid voltages as illustrated in Figure 5B(a), the positive-sequence components of the grid voltages extracted by the SOGI method are sinusoidal and balanced. The *dq*-axis grid

voltage components are illustrated in Figure 5B(c). Also, the grid phase angle grid is well estimated under unbalanced and distorted grid voltage, as shown Figure 5B(d).

By applying the proposed method (PIR controller), the control performance of the grid-side converter is seen in Figure 6, in which the grid currents (i_{gabc}) are almost sinusoidal as illustrated in Figure 6(b). The grid current components in the dq-axis (I_{dqe}) are regulated as shown in Figure 6(c). Figure 6(d) shows the DC-link voltage (V_{dc}), which is kept constant around 1.2 kV (V_{dc}^{*}). As can be clearly seen, the percentage of the DC-link voltage error is just 0.3 %.

Figure 7 shows the fast Fourier transform (FFT) spectra of the grid currents in which unbalanced and distorted voltages with the harmonic components of fifth and seventh orders are illustrated in Figure 6(a). With the proposed method, it is seen from Figure 7(c) to (d) that the grid currents mostly contain the fundamental components only, with small total harmonic distortion (THD) factor. The THD factors of the currents in phase A, phase B and phase C which are calculated thanks to the available THD function on Simview of PSIM software are 1.206%, 1.202 % and 1.205%, respectively.

The control performance of the generator is shown in Figure 8. Figure 8(a) shows the generator speed (ω_r), which follows its reference (ω_r^{*}) well. The power conversion coefficient (C_p) is illustrated in Figure 8(b). The generator currents in dq-axis (I_{dqse}) are shown in Figure 8(c), in which the d-axis current (I_{dse}) is regulated to be zero. Figure 8(d) shows the active power (P_{gen}) generated from the PMSG.

The effectiveness of the proposed control scheme for the grid PWM converter with the LCL filters is investigated in the case of the step-wise wind speed variation and under the distorted grid voltage conditions. When the wind speed changes from 7.5 m/s to 9.2 m/s at 4 s and returns to 7.5 m/s at 5 s as illustrated in Figure 9(a), the generator power has the same waveform as wind speed as shown in Figure 9(c). In this case, the DC-link voltage is still kept close to rated value as illustrated in Figure 9(b), in which the voltage overshoot is less than 1%, compared with its reference. In case of the distorted grid voltage as shown in Figure 9(d) and (e), the grid currents are still controlled well, which are sinusoidal and balanced as shown in Figure 9(f) and (g).

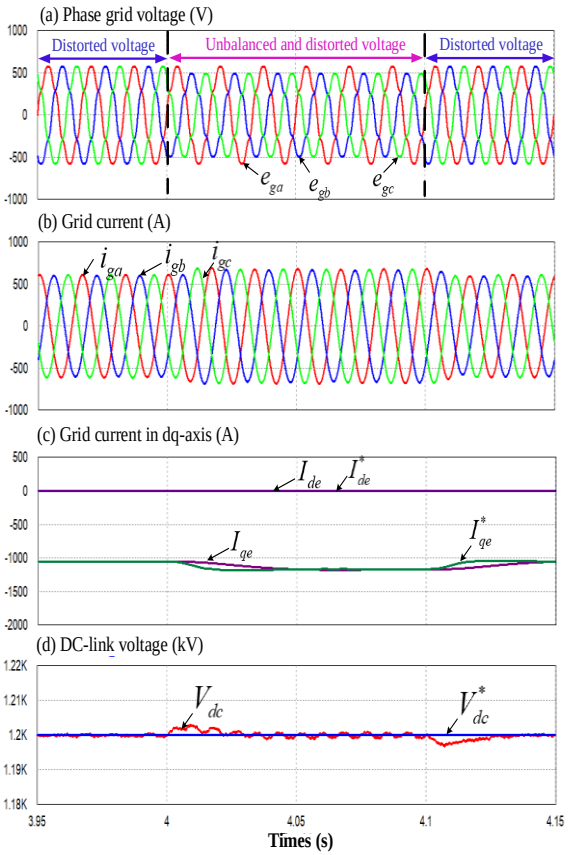

Figure 6. *Control performance of grid-side converter in unbalanced and distorted grid voltage*

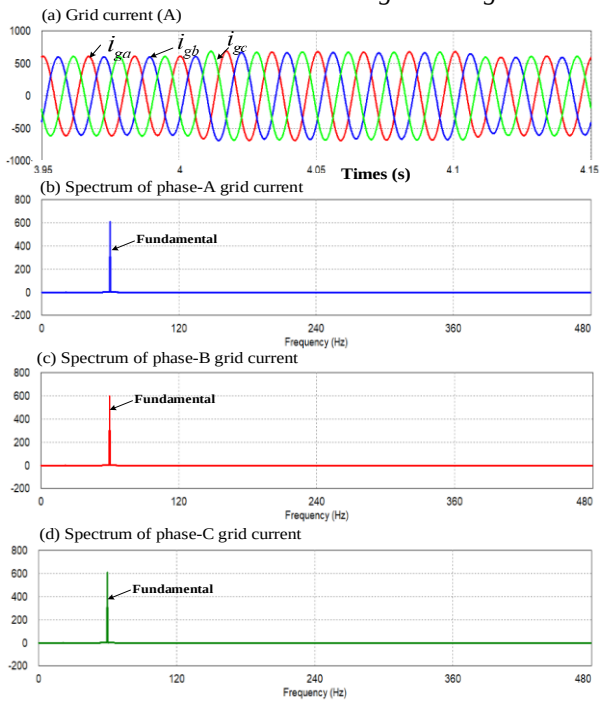

Figure 7. *FFT spectra of grid currents in unbalanced and distorted grid voltage.*

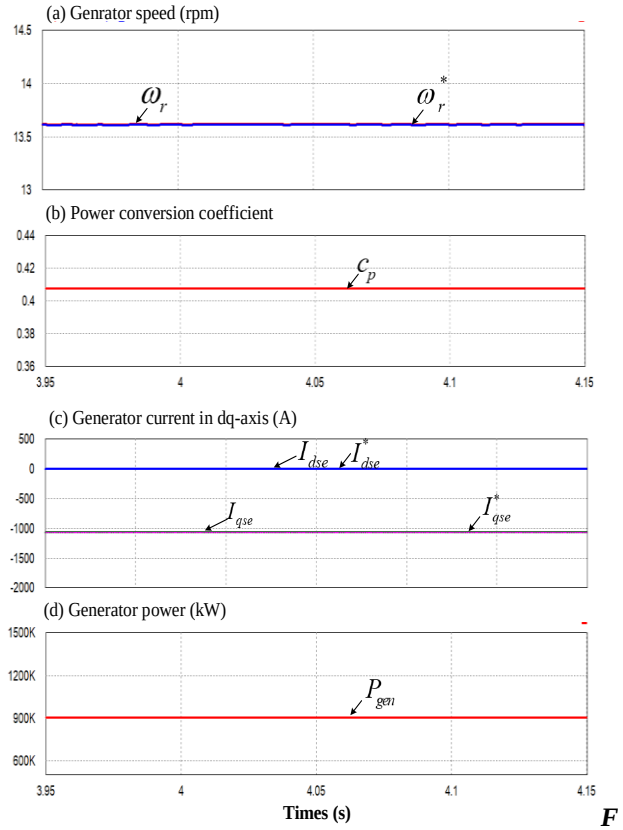

Figure 8. *Control performance of generator in unbalanced and distorted grid voltage*

VII. CONCLUSION

The paper proposes a control scheme for a grid-connected voltage-source converter of PMSG wind turbine system under unbalanced and distorted grid voltage. With the proposed control scheme, the current control performance of the grid converter has been improved significantly, in which the unbalanced and high-order harmonic components of the grid current are controlled to nearly zero by the PIR regulators. Thus, the currents feeding to the grid are almost sinusoidal and balanced regardless of the grid voltage distortion and unbalance. The validity of the proposed scheme has been verified by the simulation results.

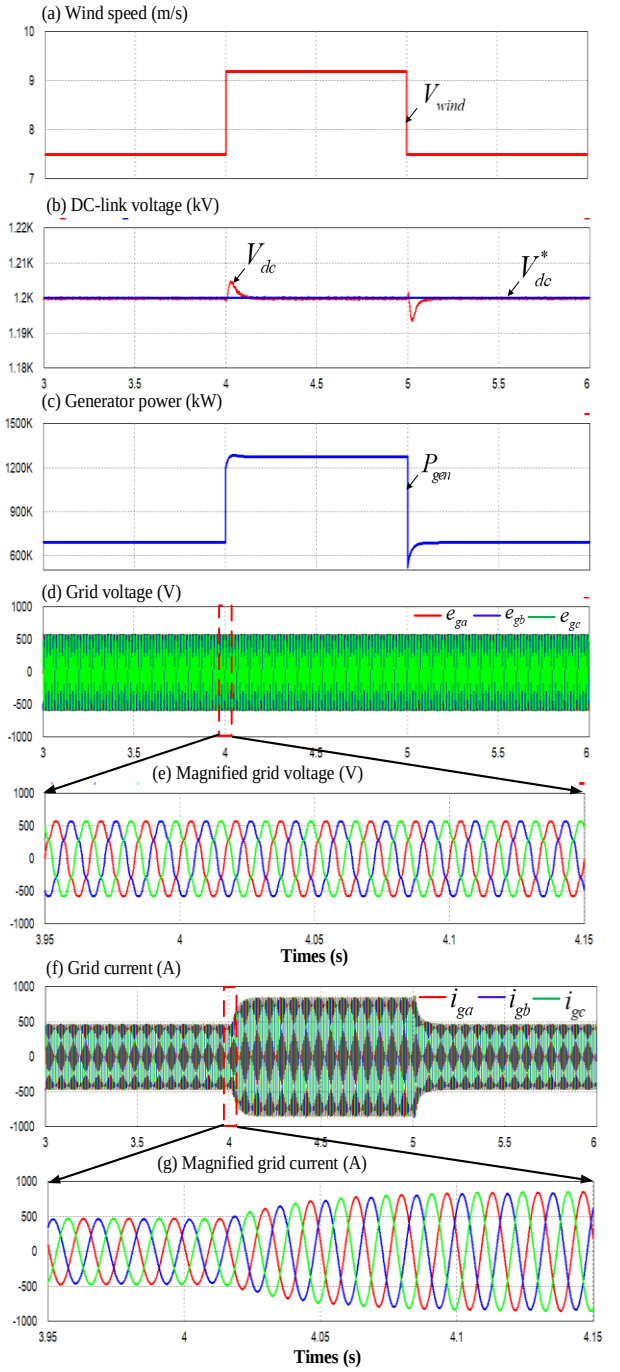

Figure 9. *Responses of proposed control scheme in stepwise wind speed variation*

REFERENCES

[1] Hatua K., Jain A. K., Banerjee D., and Ranganathan V. T. (2012), "Active damping of output LC filter resonance for vector-controlled VSI-fed AC motor drives", *IEEE Transactions on Industrial Electronics*, Vol. 59**,** No. 1, pp. 334-342.

[2] Liserre M., Teodorescu R., and Blaabjerg F. (2006), "Stability of photovoltaic and wind turbine grid-connected inverters for a large set of grid impedance values", *IEEE Transactions on Power Electronics*, Vol. 21, No. 1, pp. 263-272.

[3] Zhang X., Pan W., Liu Y., and Xu D. (2012), "Improved grid voltage control strategy for wind farm with DFIG connected to distribution networks", *Journal of Power Electronics*, Vol.12, No. 3, pp. 495-502.

[4] Song H.-S. and Nam K. (1999), "Dual current control scheme for PWM converter under unbalanced input voltage conditions", *IEEE Transactions on Power Electronics*, Vol. 46, No. 5, pp. 953-959.

[5] Lee K., Jahns T. M., Lipo T. A., Blasko V., and Lorenz R. D. (2009), "Observer-based control methods for combined source-voltage harmonics and unbalance disturbances in PWM voltage-source converters", *IEEE Transactions Industry Applications*, Vol. 45, No. 6, pp. 2010-2021.

[6] Kaura V. and Blasco V. **(**1997), "Operation of a Phase Locked Loop System under Distorted Utility Conditions",

IEEE Transactions on Industry Applications, Vol. 33, No. 1, pp. 58–63.

[7] Chung S. (2000), "A Phase Tracking System for Three Phase Utility Interface Inverters", *IEEE Transactions on Power Electronics*, Vol. 15, No. 3, pp. 431–438.

[8] Rodrigue P., Pou J., Bergas J., Candela J. I., Burgos R.P. and Boroyevich D. (2007), "Decoupled Double Synchronous Reference Frame PLL for Power Converters Control", *IEEE Transactions on Power Electronics*, Vol. 22, No. 2, pp. 584–592.

[9] Adolfo R. López-Núñez, J. D. Mina, J. Aguayo and G. Calderón (2016), "Proportional Integral Resonant Controller for Current Harmonics Mitigation in a Wind Energy Conversion System", 2016 13th International Conference on Power Electronics (CIEP), pp. 232–237.

[10] Phan V. and Lee H. (2011), "Control strategy for harmonic elimination in standalone DFIG applications with nonlinear loads", IEEE Trans. Power Electron., vol. 26, no. 9, pp. 2662–2675, Sep. 2011.

[11] Yaoqin Jia, Jiqian Zhao, and Xiaowei Fu (2014), "Direct Grid Current Control of LCL-Filtered Grid-Connected Inverter Mitigating Grid Voltage Disturbance", *IEEE Transactions on Power Electronics*, Vol. 29, No. 3, pp. 1532-1541.

[12] Amr Radwan and Yasser Ibrahim (2015), "Assessment and performance evaluation of DC-side interactions of voltage–source inverters interfacing renewable energy systems", *Sustainable Energy, Grids and Networks*, Vol. 1, pp. 28-44.

[13] Dannehl J., Liserre M., and Wilhelm F. (2011), "Filter-based active damping of voltage source converters with LCL filters", *IEEE Transactions on Industrial Electronics*, Vol. 58, No. 8, pp. 3623-3632.

[14] Alepuz S., Monge S. B., Bordonau J., Velasco J. A. M., Silva C. A., Pontt J., and Rodriquez J. (2009), "Control strategies based on symmetrical components for grid-connected converters under voltage dips", *IEEE Transactions on Industrial Electronics*, Vol. 56, No. 6, pp. 2162-2173.

[15] Rodriguez P., Luna A., Aguilar R.S.M., Otadui I.E., Teodorescu R., Blaabjerg F. (2012), "A stationary reference frame grid synchronization system for three-phase grid-connected power converters under adverse grid conditions", *IEEE Transactions on Power Electronics*, Vol. 27, No. 1, pp. 99-112.

[16] Park J.-S., Lee D.-C., and Van T. L. (2013), "Advanced singlephase SOGI-FLL using self tuning gain based on fuzzy logic", *Proceedings of 2013 IEEE ECCE Asia*, pp. 1282-1288.

[17] Teodorescue R., Liserre M., and Rodriguez P., -Grid converters for photovoltaic and wind power systems, Chapter 8, 2011, *Wiley*, United Kingdom.

CẢI TIẾN LƯỚI TÍCH HỢP CHO HỆ THỐNG TUA BIN GIÓ PMSG THEO KHOẢNG CÁCH ĐIỆN ÁP LƯỚI.

Tóm tắt: Trong bài báo này, một phương pháp điều khiển nâng cao cho bộ chuyển đổi nguồn điện áp nối lưới của hệ thống tua bin gió dùng máy phát điện đồng bộ nam châm vĩnh cửu (PMSG) trong điều kiện điện áp lưới không cân bằng và bị méo dạng. Với phương pháp được đề xuất, các bộ điều chỉnh dòng điện lưới dựa trên bộ điều khiển tỉ lệ tích phân và cộng hưởng (PIR) được áp dụng để giảm thiểu sự biến dạng dòng điện chạy vào lưới điện. Hiệu quả của các phương pháp đề xuất được xác minh bằng kết quả mô phỏng cho hệ thống tua bin gió dùng máy phát PMSG công suất 2 [MW].

Từ khóa – bộ chuyển đổi lưới, không cân bằng và méo dạng, điều khiển tích phân và cộng hưởng, tua bin gió.

Van Tan Luong was born in Vietnam. He received the B.Sc. and M.Sc. degrees in electrical engineering from Ho Chi Minh City University of Technology, Ho Chi Minh city, Vietnam, in 2003 and 2005, respectively, and Ph.D. degree in electrical engineering from Yeungnam University, Gyeongsan, South Korea in 2013. Currently, he is working at Department of Electrical and Electronics Engineering, Ho Chi Minh city University of Food Industry. His research interests include power converters, machine drives, wind power generation, power quality and power system

Ho Nhut Minh was born in Vietnam in 1987. He received his undergraduate degree in 2010, major in Electronics & Telecommunications Engineering from University of Technical Education of Ho Chi Minh City. In 2014, he received the Master of Telecommunication Engineering Degree from Posts and Telecommunications Institute of Technology, Ho Chi Minh City Campus. He is working at Department of Electrical and Electronic Engineering, Posts and Telecommunications Institute of Technology, Ho Chi Minh City Campus, VietNam.